Effects of polymer chains on structure and dynamics of supercooled water in poly(vinyl alcohol)

Yoshinori Tamai
Venture Business Laboratory, Kobe University, Kobe 657-8501, Japan

Hideki Tanaka
Department of Chemistry, Faculty of Science, Okayama University, Tsushima-naka, Okayama 700-8530, Japan

(Received 12 June 1998; revised manuscript received 7 December 1998)

Molecular-dynamics simulations for poly(vinyl alcohol) hydrogels have been carried out in a wide temperature range 150–400 K to examine effects of polymer chains on structure and dynamics of supercooled water in hydrogels. A fragile-strong character of water under perturbations of polymer chains is examined. Polymer chains affect the fragile-strong character of water, which is manifested in temperature dependences of potential energy, translational diffusion coefficient, and orientational relaxation time. Water coexisting with polymer has a rather stronger character in the strong-fragile classification than that in pure water. Structure and dynamics of water in hydrogels are significantly altered by the slow dynamics of polymer chains, as well as the structure and dynamics of hydrogen-bond networks. [S1063-651X(99)04405-0]

PACS number(s): 61.20.Lc, 61.20.Ja, 61.25.Hq, 64.70.Ja

I. INTRODUCTION

We have performed molecular-dynamics (MD) simulations of hydrogels and examined both structural and dynamical aspects [1,2]. Special care was taken of the interplay between water and polymer segmental motions. We found that polymer chains significantly affect hydrogen-bond structures and dynamics of water in hydrogels. Compartmentation of water molecules in hydrogels changes the character of water from a bulk one.

Water exhibits various anomalies in thermodynamic response functions such as heat capacity and isothermal compressibility [3,4]. Those properties in a supercooled state tend to diverge when approaching T_s, 228 K [5], although water always freezes to ice at a temperature higher by a few degrees than T_s. Tanaka [6,7] demonstrated that the potential energy drops significantly at a certain temperature and proposed a phase diagram which is different in the location of the second critical point from that suggested by Stanley and co-workers [8,9]. According to the phase diagram proposed by Tanaka, the TIP4P water undergoes a first-order phase transition between low- and high-density liquids (LDL and HDL) at 213 K under ambient pressure; the density jumps discontinuously at 213 K. Sciortino *et al.* [10], however, questioned this interpretation; they argued that the density change is continuous. In spite of the apparent difference in the existence of the continuous path from normal supercooled water to LDL, the underlying idea to account for those anomalous properties of water is that the phase equilibrium between LDL and HDL is responsible for those anomalous properties, apart from the location of the second critical point. But we will not address in the present paper the topic as to where there is a critical point in a temperature-pressure plane.

The divergent character is suppressed and water is cooled down to the glass transition temperature when alcohol or hydrogen peroxide is dissolved [3]. A possible explanation is that LDL structure cannot exist with those solutes because of steric factor, i.e., differences in geometry and the number of hydrogen bonding sites. The temperature dependence of the viscosity (and rotational relaxation time) is described by the Vogel-Tammann-Fulcher (VTF) equation, which means that the aqueous solution belongs to a fragile liquid over a wide range of temperature [11–13]. Water molecules coexisting with polypeptide have a different temperature dependence of the relaxation time of rotational motions and are considered to be rather strong liquids [14]. Angell suggested that this type of behavior may be common to all hydrophilic polymers hence to a large number of biopolymer systems [11]. Some of the evidence were also observed in our previous simulation study for poly(vinyl alcohol) (PVA) hydrogel [15]. It is important to investigate why water changes its dynamic characters by changing coexistent solute species from small hydrophilic molecules to polymers.

The glass transition phenomena and properties of supercooled liquids and glasses have long been studied but have not yet been understood completely [12,13,16]. Glass-forming systems have canonical features: non-Arrhenius behavior (fragility), nonexponential relaxation, and nonlinearity of relaxation (nonergodic). Specific heat and thermal expansion coefficients exhibit discontinuities at the glass transition temperature T_g, below which configurational rearrangements are extremely slow. It is expected that structure and dynamics of water in hydrogels are affected by a significant change in polymer segmental motions at T_g of neat polymer. It is very interesting to examine the effects of polymer chains on the structure and dynamics of water since those have a close relation to cryopreservation.

In the present paper, the structure and dynamics of supercooled water in PVA hydrogel are investigated through MD simulations of rather long time runs in a wide temperature range 150–400 K. We investigate structure and dynamics of water, which is significantly perturbed by polymer chains.

II. MD SIMULATIONS

MD simulations are performed for pure water and hydrogel models of PVA. Samples are listed in Table I. The

TABLE I. Degree of polymerization x, number of water molecules n_w, and water content c_w of each sample.

Sample	x	n_w	c_w (wt %)
PVA/water	161	150	27.5
PVA/water	81	199	50.0
Pure water		216	100

amount of water in the hydrogels c_w is 27.5 or 50.0 wt % of the hydrated polymer. Here, the ratio of water to polymers is 0.38:1 or 1:1, respectively. PVA is modeled as H—[—CH_2—CH(OH)—]$_x$—CH_3 with degree of polymerization $x=81$ or 161. The fraction of meso dyads is 0.5 (atactic). A polymer chain is confined in a unit cell with 199 or 150 water molecules under the periodic boundary condition. The chain may be entangled with its image chains. The AMBER/OPLS (optimized potential for liquid simulations) [17,18] force field is used for the polymer, and the TIP4P [19] for water. The united atom approximation is applied for —CH_3, —CH_2—, and >CH— groups, each of which is treated as a single interaction site. Nonbonded potentials are truncated smoothly at 9 Å. The long-range correction for Lennard-Jones part is made. Initial structures are obtained by the same method as described elsewhere [1,2]. The equations of motion are solved by the Verlet algorithm with a time step of 0.5 or 1 fs. The bond angles CH—O—H of PVA and all the bond lengths are constrained by the SHAKE algorithm. The TIP4P water is treated as a rigid molecule by the SHAKE vectorial constraint method [20]. Simulations are performed at various temperatures (150–400 K) and a fixed pressure (0.1 MPa) using the Nosé-Andersen's constant temperature-pressure method [21–23]; the density of the system is allowed to fluctuate. A cubic periodic cell is used for the simulations of pure water. For the simulations of hydrogels a rectangular cell is used; three cell lengths are allowed to fluctuate independently. The simulations are performed sequentially from higher temperatures to lower temperatures according to the stepwise cooling schedule shown in Fig. 1. Equilibration runs of 0.2–0.5 ns are inserted between two simulations at successive temperatures. In this condition, the effective cooling rate is approximately 10^{10} K/s. After equilibrium has been reached, the density fluctuates around an average value. The sampling time ranges from 1 to 40 ns for each temperature. During sampling, no systematic drift is observed in the time evolution of potential energy, as shown in our previous study [15]. Therefore, systems are considered to be equilibrated at least for static properties, such as density or potential energy. Trajectories and velocities of atoms are recorded every 500 steps on disk files for later analyses.

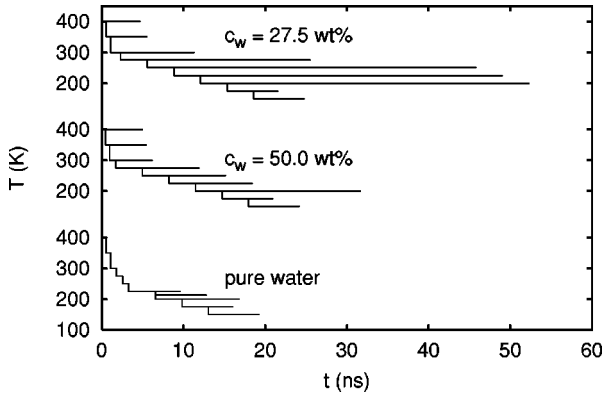

FIG. 1. Schedule of stepwise cooling procedures for MD simulation of PVA hydrogel and pure water. Simulations are started at 400 K for each sample which is cooled down to 150 K along with the schedule shown by stepwise solid lines. As shown by horizontal lines, further sampling runs are performed at each temperature.

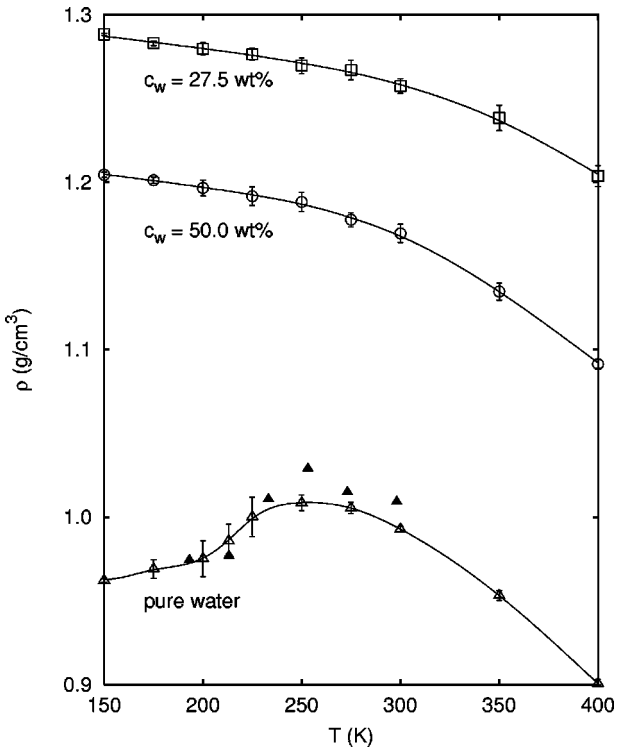

FIG. 2. Temperature dependence of the density of PVA hydrogels with water content $c_w=27.5$ wt % (square) and 50.0 wt % (circle), and that of pure water (triangle). Standard fluctuations are shown by vertical lines. The solid curves (splines) are guides to the eye. The simulation results of Tanaka are also plotted (filled triangle).

In order to extract purely structural information, the thermally excited vibrational motions are removed from a set of configurations generated by MD simulations, which are called instantaneous (I) structures. I structures are quenched to the corresponding local potential energy minimum structures, called Q structures. Q structures are obtained by applying the steepest descent energy minimization with the same constraint condition as the MD simulation using the gradient-SHAKE method [24]. Relaxation of polymer chains in hydrogels, diffusion coefficient and reorientational relaxation time of water, and distribution and dynamics of hydrogen bonds are examined.

Simulations are performed on DEC Alpha and HP 700 series workstations and on a CRAY Origin 2000 parallel computer, using the molecular-simulation program PAMPS we coded.

III. RESULTS AND DISCUSSION

A. Thermodynamic properties of water

Temperature dependences of density are given in Fig. 2. The individual point is an average over total sampling runs at

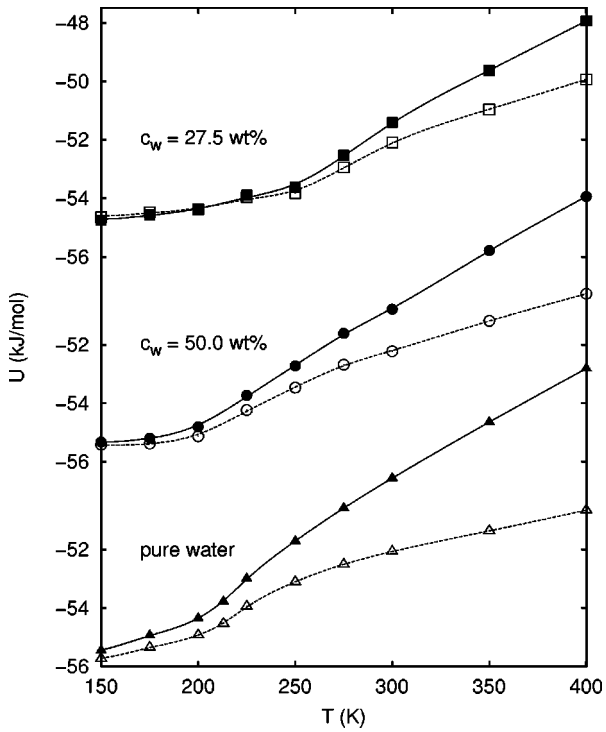

FIG. 3. Temperature dependence of the potential energy of a water molecule in I structures (filled symbols) and that in Q structures (open symbols). Water-water and water-polymer interactions are included. Standard fluctuations are smaller than the symbol. The solid curves (splines) are guides to the eye.

each temperature. The density of pure water shows a maximum. An abrupt change is found around 210 K, where the density fluctuation is also large. Since present simulations are performed with a small number of molecules and isothermal-isobaric ensembles, the change in density becomes facile in the vicinity of the critical point where the fluctuation becomes large, as shown in Fig 2. Harrington *et al.* [25] reported the existence of a liquid-liquid phase transition for the ST2 model of liquid water; state points inside the coexistence region separate into two phases. Owing to a large number of molecules (1728) and an isochoric system in their simulation, low- and high-density regions coexist in the basic simulation cell. In our study, on the other hand, the whole simulation cell takes low- and high-density states alternately with a long period at around 210 K because of isobaric condition and a small number of molecules: Even though the sharp change in the thermodynamic limit is expected, it is somehow blurred in the present system size. Therefore, we will not refer here to a definite conclusion on the discontinuity or continuity of water.

For PVA hydrogels, no gaps are found in the density plot against temperatures. The magnitude of the density fluctuation decreases monotonically with decreasing temperature.

The potential energies of water for both I and Q structures are plotted in Fig. 3. The potential energy of water is given by the sum of water-water and water-polymer interactions. The I-structure energy is the sum of Q-structure energy plus thermal energy, the latter of which is decomposed further into harmonic and anharmonic vibrational energy. To remove a trivial temperature dependence, the harmonic energy $3RT$ is subtracted from the I-structure energy in the plot. The difference between two lines (I- and Q-structure energy) corresponds to the contribution of the anharmonic energy. The potential energy of the Q structure for supercooled water decreases with declining temperature. It has been argued that in the strong-fragile classification, a fragile character arises from the anharmonic nature of the potential energy surface [12,13]. This implies that water in the pure state and polymer solutions with high water contents have a fragile character at higher temperatures. As the concentration of the polymer increases, the anharmonic energy (the difference between two lines) decreases. This smaller anharmonic energy indicates that the strong character increases with polymer concentration [12]. The decrease in anharmonicity in the system of lower water contents implies that the one-to-one nature of polymer-water hydrogen bonds dominates the cooperative nature of water-water hydrogen bonds.

B. Translational diffusion of water

Figure 4 shows logarithmic plots of the mean-square displacements (MSD's) of water. The MSD lines shorter than 10 ps are obtained from *NVT* MD simulations at average densities of each temperature in order to calculate short-time correlations correctly. Overshoots are observed at low temperature, which is similar to the results of Gallo *et al.* [26]. For pure water, the normal diffusion (Einstein) regime is achieved above 175 K; the slopes of the figure become unity after the root-mean-square displacements exceed approximately the radius of a water molecule. The normal diffusion regime is achieved above 200 K for the sample of $c_w = 50.0$ wt%. Water molecules diffuse on the average almost its diameter during 40 ns of MD runs even at 200 K in the samples of $c_w = 27.5$ wt%. Therefore, analysis of water dynamics from the present simulation is justified above 200 K. The anomalous diffusion (non-Einstein) regime persists for a long time at low temperature, especially in the sample of $c_w = 27.5$ wt%, as in the case of the diffusion of small penetrants in a pure polymer matrix [27]. The motion of water is highly hindered by strong polymer-water interactions, especially the sample of $c_w = 27.5$ wt%.

A series of trajectories at each temperature are divided into five intervals, from which self-diffusion coefficients D_s are calculated by the least-squares fit. Figure 5 shows D_s of water above 200 K averaged over five intervals. The values of D_s for pure water are approximately two times larger than those calculated by the SPC/E potential model [2]. By using the TIP4P model, mobility is slightly overestimated. Provided that the Stokes-Einstein formula is valid in this temperature range, a systematic decrease of slope in the Arrhenius plot indicates that water is a fragile liquid. It is also revealed that water becomes stronger with decreasing water contents in hydrogels. This is consistent with the above conclusion derived from the magnitude of the anharmonic energies.

C. Nonexponentiality of relaxation

The orientational time correlation function is defined as

$$C_1(t) = \langle \mathbf{u}(t_0) \cdot \mathbf{u}(t+t_0) \rangle, \tag{1}$$

where $\mathbf{u}(t)$ denotes a unit vector along the dipole vector of a

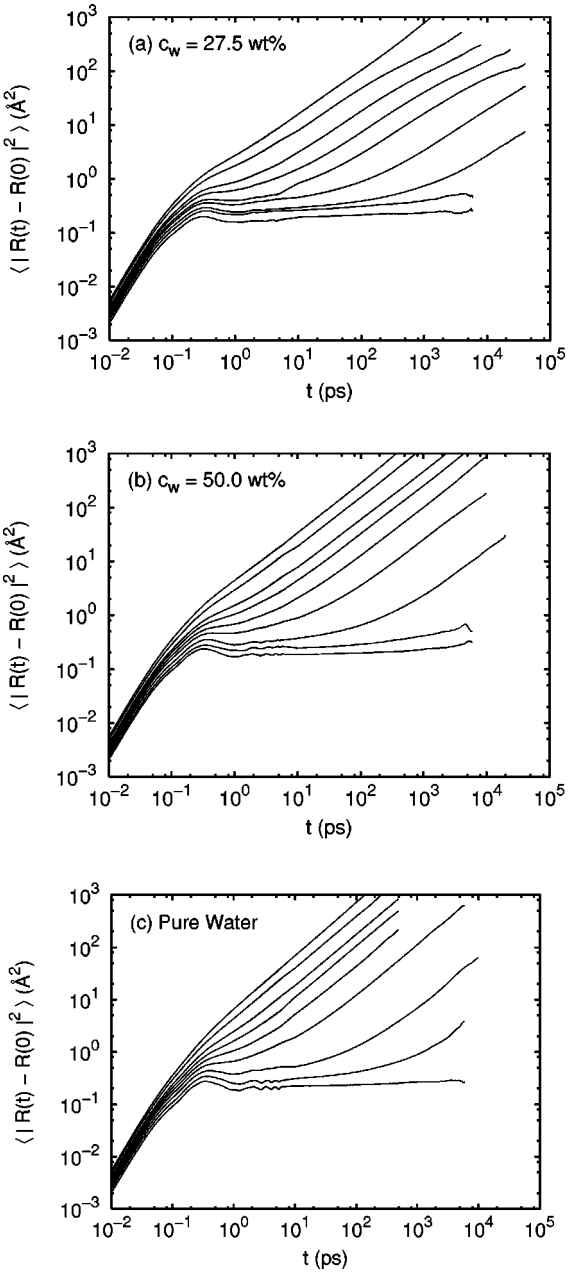

FIG. 4. Mean-square displacement (MSD) of water in PVA hydrogels of water content $c_w = 27.5$ wt % (a) and 50.0 wt % (b) and that in pure water (c). Each line from upper to lower represents MSD at 400, 350, 300, 275, 250, 225, 200, 175, and 150 K, respectively.

water molecule, $\boldsymbol{\mu}_{\mathrm{dip}}$. This is related to a dielectric relaxation and is expressed by a single exponential (Debye) type for pure water at room temperature. It deviates, however, from the single exponential function. In the supercooled state, the correlation functions $C_1(t)$ are well fitted to the following stretched exponential, or Kohlrausch-Williams-Watts (KWW), function

$$C_1(t) = \exp[-(t/\tau)^{\beta}]. \tag{2}$$

If the correlation function which is well described by Eq. (2) with small β is fitted by the superposition of several exponential functions with $\beta = 1$ (Debye type), the system has

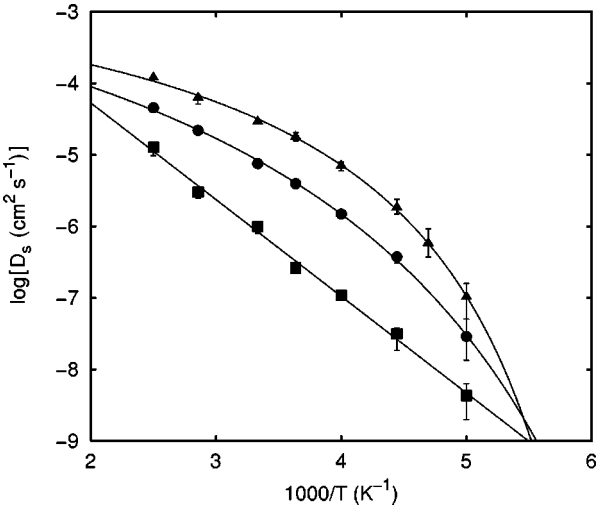

FIG. 5. Diffusion coefficient D_s of water in PVA hydrogels of water content $c_w = 27.5$ wt % (square) and 50.0 wt % (circle) and that in pure water (triangle) (logarithm to base 10). Each point is an average value of diffusion coefficients which are obtained from five subsets of MD trajectories. Error bars are based on minimum and maximum of five D_s values at each temperature.

various relaxation times. Non-Debye response functions are a ubiquitous dynamical feature across supercooled liquids and amorphous polymers in their α-relaxation regime. Reorientational relaxation time τ and exponent β $(0 < \beta < 1)$ are determined by a nonlinear least-squares method using five subsets of MD trajectories at each temperature. The lines of $C_1(t)$ are successfully fitted to Eq. (2) above 200 K, though fitting becomes difficult at temperatures lower than 200 K because of the extremely slow relaxation. Therefore, we will discuss the strong-fragile character of water on the basis of the fitted relaxation times at temperatures above 200 K.

The average values of stretching exponent β obtained by least-squares fitting are listed in Table II. The small values of β, ~ 0.35, in $c_w = 27.5$ wt % hydrogel suggests a broad distribution of relaxation time, which is also reported for proteins: $\beta = 0.2 - 0.4$.

D. Non-Arrhenius behavior of relaxation time

The reorientational relaxation times τ of water molecules averaged over five subsets are shown in Fig. 6 with experi-

TABLE II. Stretching exponent β of the KWW function [Eq. (2)]. The values are average ones calculated from five subsets of MD trajectories at each temperature.

T (K)	$c_w = 27.5$	$c_w = 50.0$	$c_w = 100$
200		0.50	0.69
213			0.75
225	0.39	0.46	0.79
250	0.29	0.39	0.77
275	0.30	0.41	0.77
300	0.30	0.46	0.78
350	0.37	0.56	0.79
400	0.47	0.63	0.80
Av.	0.35	0.49	0.77

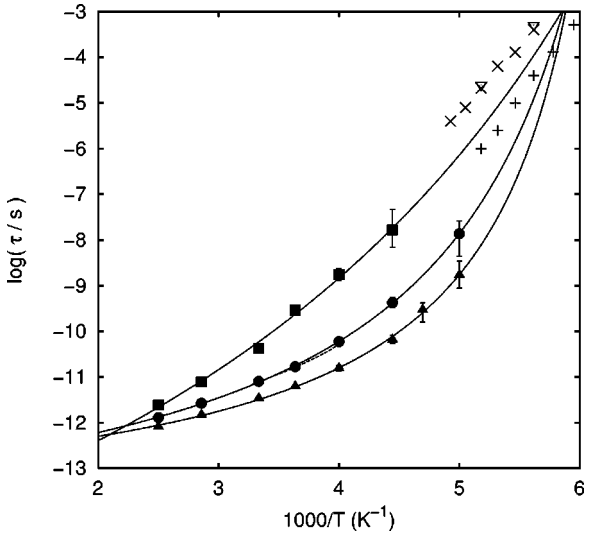

FIG. 6. Reorientational relaxation time τ of water in PVA hydrogels of water content $c_w = 27.5$ wt % (square) and 50.0 wt % (circle) and that in pure water (triangle) (logarithm to base 10). Each point is an average value of relaxation times which are obtained from five subsets of MD trajectories. Error bars, which are based on minimum and maximum of five τ values at each temperature, are smaller than symbols for most of the points. The data points are fitted to the VTF equation [Eq. (3)]. Experimental data of the dielectric relaxation time are also plotted for pure water (- - -) (Bertolini *et al.*) and water in poly(2-hydroxyethyl methacrylate) of water content $c_w = 24$ (∇), 32 ($\times$), and 51 wt % (+) (Xu *et al.*)

mental data. Relaxation time of water is more than one order smaller than that of the side chain motion of PVA, and three to four orders smaller than that of the main chain [28]. The motion of water molecules is highly hindered by the slow motion of polymer chains. The data points are well fitted by the modified VTF equation for the relaxation time

$$\tau(T) = \tau_0 \exp\left(\frac{DT_0}{T - T_0}\right), \tag{3}$$

where τ_0, D, and T_0 are fitting parameters. The temperature dependence of τ for pure water agrees with experimental data [29], though mobility is systematically overestimated. This may be owing to a character of the potential model TIP4P (diffusion coefficients are also overestimated). Experimental values of the dielectric relaxation time of water in poly(2-hydroxyethyl methacrylate) (PHEMA) hydrogel of water content $c_w = 24$, 32, and 51 wt % [30] lie above the VTF lines of our simulation results. Experimental and simulation data could be smoothly connected, considering the difference in the observation time between them.

For pure water, deviation from the Arrhenius behavior is obvious; water is classified into fragile liquids. In PVA hydrogels, the temperature dependence of τ approaches the Arrhenius type with decreasing water content. Best fitted values of the fitting parameters τ_0, D, and T_0 are listed in Table III. As is clear from the strength parameter D, water surrounded by PVA chains is rather strong at low water content. Slow dynamics of polymer chains affect dynamic properties of water through strong hydrogen bonds between polymer and water in such a way as to remove complicated cooperative motions and to approach a relaxation of the Arrhenius type. Green *et al.* [14] determined fragility for model homopeptide poly-L-asparagine ($c_w = 15.5$ wt %) from scan rate dependence experiments by the differential scanning calorimetry. The VTF plot of the relaxation times calculated from the fragility parameter shows even stronger behavior than that of polyisobutylene (PIB), which is known as the strongest chain polymer ($D \simeq 20$). Angell suggested that this type of behavior may be common to all hydrophilic polymers [11]. Our present result supports this suggestion. The correlation between nonexponential relaxations and non-Arrhenius behavior is discussed by Böhmer *et al.* [31]. Except for orientational glasses and monohydric aliphatic alcohols, a distinct but broad correlation of non-Debye behavior with non-Arrhenius relaxations is found.

TABLE III. Fitted parameters of the modified VTF equation [Eq. (3)].

c_w (wt %)	D	T_0 (K)	$\log_{10}(\tau_0/\mathrm{s})$
27.5	23	92	−14.6
50.0	5.3	139	−13.1
100	3.3	148	−12.9

The ideal glass transition temperature T_0, at which relaxation time diverges, coincides with the Kauzmann temperature and should lie below T_g by an amount which depends on the parameter D. In our simulation, the value of T_0 for pure water is a little higher than the experimental T_g, 136 K. Referring to the MSD of water shown in Fig. 4(c), water molecules no longer diffuse translationally at 150 K. The T_g of water lies around 170 K in the simulation of the present condition (the observation time $\sim 10^{-8}$ s, the effective cooling rate $\sim 10^{10}$ K/s).

E. Structure of water in the vicinity of hydrogel

Snapshots of PVA hydrogel shown in our related paper [28] give an impression of the rather distinct structure of hydrogel. Water molecules are classified into three categories: (1) those around hydrophilic groups, (2) those around hydrophobic groups, and (3) the bulk region. The hydrophilic region is defined so as to cover the inner region up to the first peaks of the radial distribution functions $g(r)$ of water oxygen atoms around —OH groups. The hydrophobic region is similarly defined for hydrophobic groups: >CH—, —CH_2—, and —CH_3. The regions which belong to both regions (1) and (2) are incorporated in region (1). The bulk region is defined as a region outside regions (1) and (2) (out of the first hydration shells).

Table IV lists the average numbers of water molecules in each region. In the present samples, 93% ($c_w = 27.5$ wt %) or 64% ($c_w = 50.0$ wt %) of water molecules reside in the

TABLE IV. Average number of water molecules in each region of hydrogels.

c_w (wt %)	Hydrophilic	Hydrophobic	Bulk
27.5	112.1	28.3	9.6
50.0	86.7	42.0	70.3

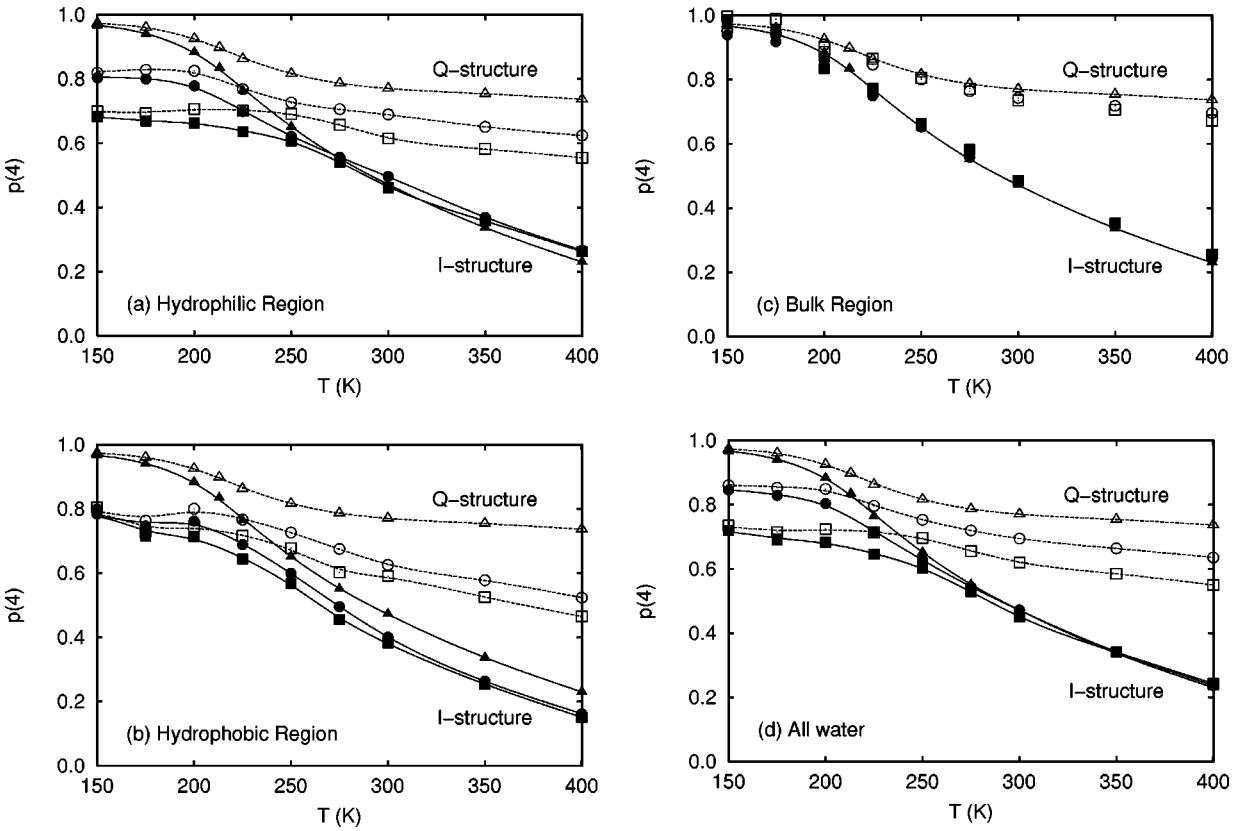

FIG. 7. Fractions of water molecules which have four hydrogen bonds in I structures (filled symbols) and that in Q structures (open symbols) of PVA hydrogels of water content $c_w = 27.5$ wt % (square) and 50.0 wt % (circle): (a) water around hydrophilic groups, (b) water around hydrophobic groups, (c) water out of the first hydration shell, and (d) all water molecules. Data for pure water is also plotted in the figures (triangle).

first hydration shell. In the system of $c_w = 27.5$ wt %, narrow interstices contain water molecules, several of which bridge two —OH groups of PVA. On the other hand, the bulk region forms a *water ball* in the sample of $c_w = 50.0$ wt %. It is expected that water in the latter preserves the bulk nature to a certain extent.

F. Structure of hydrogen-bond networks

With decreasing temperature, the network structure of hydrogen bonds for water is more enhanced; defects of the tetrahedral network structure decrease. A water molecule forms four hydrogen bonds in ice. Therefore, the fraction of water molecules which have four hydrogen bonds, $p(4)$, could be a measure of the perfectness of the hydrogen bonds. Figure 7 shows the temperature dependence of $p(4)$ in each region defined above. Hydrogen bonds are defined by a geometry criterion, in the same manner as our previous study [1,2]. In pure water, $p(4)$ reaches a limiting value of 0.97 at low temperature. Pure water includes only a few defects of the tetrahedral network structure below 210 K, as shown by Tanaka [7]. In the bulk region, the temperature dependence of $p(4)$ is approximately the same as that in pure water. In the hydrophobic region, $p(4)$ has an upper limit of 0.8, irrespective of water contents. In the hydrophilic region, the values of $p(4)$ strongly depend on water contents in Q structures. In I structures, the values of $p(4)$ are apparently independent of c_w above 250 K. The greater $p(4)$ at high water content in the Q structure is canceled by larger amplitude-thermal motions, which arise from the anharmonic vibrations as seen in Fig. 3. In the system of low water content, therefore, the number of configurations to form a local tetrahedral arrangement is small for the Q structure but $p(4)$ values are the same as that of pure water in the I structure.

G. Dynamics of hydrogen-bond networks

Dynamical properties of polymer chains are transferred to water molecules through hydrogen bonds between water and polymers. The dynamics of hydrogen bonds seem to play an important role in the structure and dynamics of water in hydrogels. This should be investigated in more detail. In order to examine the dynamics of hydrogen bonds, the *intermittent* hydrogen-bond autocorrelation function (HAF) [32]

TABLE V. Stretching exponent β [Eq. (2)] averaged over temperatures for the correlation functions Eq. (4) of polymer-polymer (p-p), polymer-water (p-w), and water-water (w-w) hydrogen bonds. The values of β are calculated from five subsets of trajectories at each temperature.

c_w (wt %)	p-p	p-w	w-w
27.5	0.35	0.39	0.36
50.0	0.32	0.43	0.51
100			0.64

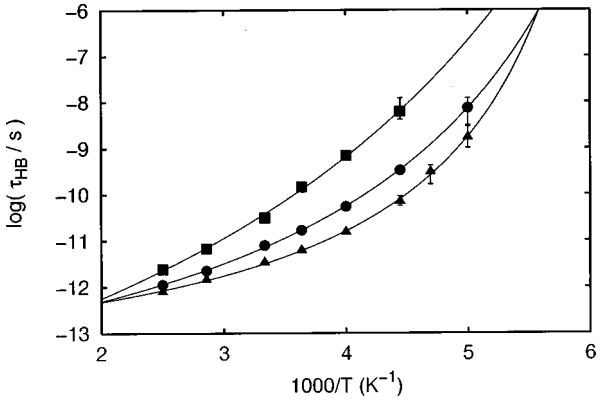

FIG. 8. Relaxation time of water-water hydrogen bonds in PVA hydrogels of water content $c_w = 27.5$ wt % (square) and 50.0 wt % (circle) and that in pure water (triangle) (logarithm to base 10). The data points are fitted to the VTF equation [Eq. (3)].

$$C_{\mathrm{HB}}(t) = \frac{\left\langle \sum_{ij} s_{ij}(t+t_0) s_{ij}(t_0) \right\rangle}{\left\langle \sum_{ij} s_{ij}(t_0) s_{ij}(t_0) \right\rangle}, \tag{4}$$

where $\langle \cdots \rangle$ means average over all possible time origins t_0, and a quantity $s_{ij}(t)$ is defined for a pair of molecules (or monomers), i and j, at time t as

$$s_{ij}(t) = \begin{cases} 1 & \text{(bonded)}, \\ 0 & \text{(nonbonded)}. \end{cases} \tag{5}$$

Only those pairs which have $s_{ij}(t_0) = 1$ are included in the sampling. This type of analysis focuses on the elapsed time until the final breakage of the bond occurs. Another definition of HAF, a *continuous* one [32], focuses on the elapsed time until the first breakage is observed. Hydrogen bonds are switched on and off repeatedly on the order of a subpicosecond by the librational motion of the molecules [2]. This time scale is reflected in the *continuous* HAF. After scores of times of bond-breaking and forming, two molecules separate from each other and the *intermittent* HAF decays gradually. The stretching exponent β and the hydrogen-bond relaxation time τ_{HB} (see Table V) is calculated by fitting Eq. (4) (*intermittent* HAF) to the KWW function [Eq. (2)].

Figure 8 shows the Arrhenius plot of τ_{HB} of water-water hydrogen bonds in PVA hydrogels and that in pure water. The figure is similar to Fig. 6 (reorientational relaxation time of water). This again implies that water becomes stronger with decreasing water contents. Figure 9 shows the τ_{HB} of polymer-water and polymer-polymer hydrogen bonds. At the T_g of polymer chains ($1000/T \sim 3.85$) [28], τ_{HB} of polymer-water hydrogen bonds in the sample of $c_w = 27.5$ wt % is comparable to the observation time $\sim 10^{-8}$ s. Since τ_{HB} in the sample of $c_w = 50.0$ wt % is one order shorter, an exchange of water molecules which are hydrogen-bonded to —OH groups of PVA occurs even below T_g of the hydrated polymer. As seen in Fig. 9, relaxation of the polymer-water hydrogen bond has a stronger nature than that of the water-water hydrogen bond.

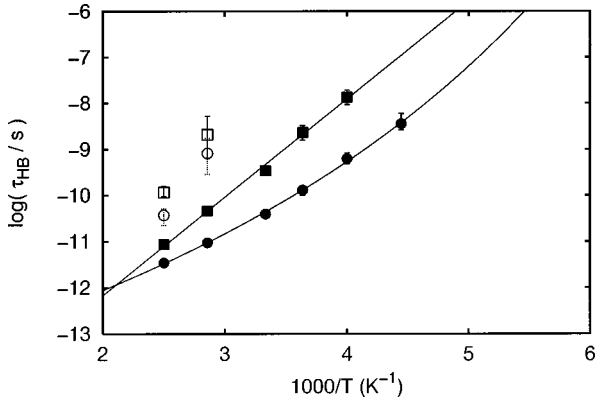

FIG. 9. Relaxation time of polymer-polymer (open symbols) and polymer-water (filled symbols) hydrogen bonds in PVA hydrogels of water content $c_w = 27.5$ wt % (square) and 50.0 wt % (circle) (logarithm to base 10). The data points are fitted to the VTF equation [Eq. (3)].

IV. CONCLUSIONS

MD simulations of rather long time runs have been carried out for PVA hydrogels and pure water in a wide temperature range 150–400 K to examine the effects of polymer chains on the structure and dynamics of supercooled water in hydrogels. A fragile-strong character of water under perturbations of polymer chains is examined. The fragile-strong character of water is affected by polymer chains, which is manifested in temperature dependences of density, potential energy, translational diffusion, and orientational relaxation time. Water in hydrogels has a rather stronger nature than that in pure water. Molecular motions of water are correlated with those of polymer. Polymer and water are mutually influenced via strong hydrogen bonds. The glass transition temperature of PVA is quite different from that of pure water. Thus, the slowing down of the PVA motion gives, necessarily, rise to slowing down of the motion of water. The large change in dynamic properties (translational diffusion and rotational relaxation), as well as the thermodynamic properties in pure water is suppressed in the hydrogel.

Water coexisting with hydrogel in the low-temperature regime seems to be different in both thermodynamic and dynamic characters from pure water since a certain amount of water in hydrogel is no longer tetrahedrally coordinated. The number of tetrahedrally coordinated water molecules do not increase even if the temperature approaches the glass transition temperature due to the steric hindrance by polymer chains. It would be worthwhile in the future to examine a difference in the nucleation mechanism between pure water and water in hydrogel, and to examine its relation to the divergence in thermodynamic response functions observed in pure water.

ACKNOWLEDGMENTS

This work was supported by the Japan Society for the Promotion of Science and by the Japan Ministry of Education. Computation time was provided by the Supercomputer Laboratory, Institute for Chemical Research, Kyoto University.

[1] Y. Tamai, H. Tanaka, and K. Nakanishi, Macromolecules **29**, 6750 (1996).
[2] Y. Tamai, H. Tanaka, and K. Nakanishi, Macromolecules **29**, 6761 (1996).
[3] C. A. Angell, in *Water: A Comprehensive Treatise*, edited by F. Franks (Plenum, New York, 1981), Vol. 7, Chap. 1.
[4] C. A. Angell, Annu. Rev. Phys. Chem. **34**, 539 (1983).
[5] R. J. Speedy, J. Phys. Chem. **96**, 2322 (1992).
[6] H. Tanaka, Nature (London) **380**, 328 (1996).
[7] H. Tanaka, J. Chem. Phys. **105**, 5099 (1996).
[8] P. H. Poole, F. Sciortino, U. Essmann, and H. E. Stanley, Nature (London) **360**, 324 (1992).
[9] P. H. Poole, F. Sciortino, U. Essmann, and H. E. Stanley, Phys. Rev. E **48**, 3799 (1993).
[10] F. Sciortino, P. H. Poole, U. Essmann, and H. E. Stanley, Phys. Rev. E **55**, 727 (1997).
[11] C. A. Angell, in *Hydrogen Bond Networks*, edited by M.-C. Bellissent-Funel and J. C. Dore (Kluwer Academic, Dordrecht, The Netherlands, 1994), pp. 3–22.
[12] C. A. Angell, Science **267**, 1924 (1995).
[13] F. H. Stillinger, Science **267**, 1935 (1995).
[14] J. L. Green, J. Fan, and C. A. Angell, J. Phys. Chem. **98**, 13 780 (1994).
[15] Y. Tamai and H. Tanaka, Chem. Phys. Lett. **285**, 127 (1998).
[16] M. D. Ediger, C. A. Angell, and S. R. Nagel, J. Phys. Chem. **100**, 13 200 (1996).
[17] W. L. Jorgensen and J. Tirado-Rives, J. Am. Chem. Soc. **110**, 1657 (1988).
[18] S. J. Weiner, P. A. Kollman, D. A. Case, U. C. Singh, C. Ghio, G. Alagona, S. Profeta, and P. Weiner, J. Am. Chem. Soc. **106**, 765 (1984).
[19] W. L. Jorgensen, J. Chandrasekhar, J. D. Madura, R. W. Impey, and M. L. Klein, J. Chem. Phys. **79**, 926 (1983).
[20] G. Ciccotti, M. Ferrario, and J.-P. Ryckaert, Mol. Phys. **47**, 1253 (1982).
[21] S. Nosé, J. Chem. Phys. **81**, 511 (1984).
[22] H. C. Andersen, J. Chem. Phys. **72**, 2384 (1980).
[23] M. Ferrario and J. P. Ryckaert, Mol. Phys. **54**, 587 (1985).
[24] Y. Duan, S. Kumar, J. M. Rosenberg, and P. A. Kollman, J. Comput. Chem. **16**, 1351 (1995).
[25] S. Harrington, R. Zhang, P. H. Poole, F. Sciortino, and H. E. Stanley, Phys. Rev. Lett. **78**, 2409 (1997).
[26] P. Gallo, F. Sciortino, P. Tartaglia, and S.-H. Chen, Phys. Rev. Lett. **76**, 2730 (1996).
[27] Y. Tamai, H. Tanaka, and K. Nakanishi, Macromolecules **27**, 4498 (1994).
[28] Y. Tamai and H. Tanaka, Mol. Simul. (in press).
[29] D. Bertolini, M. Cassettari, and G. Salvetti, J. Phys. Chem. **76**, 3285 (1982).
[30] H. Xu, J. K. Vij, and V. J. McBrierty, Polymer **35**, 227 (1994).
[31] R. Böhmer, K. L. Ngai, C. A. Angell, and D. J. Plazek, J. Phys. Chem. **99**, 4201 (1993).
[32] D. C. Rapaport, Mol. Phys. **50**, 1151 (1983).